Journal of Network Intelligence
Taiwan Ubiquitous Information
 ISSN 2414-8105
Volume **9**, Number **4**, November **2024**

Power Line Loss Reduction Based on Meta-Heuristic Algorithm in Smart IoT Environment

Hui-Na Du*

Hebi Institute of Engineering and Technology,
Henan Polytechnic University, Hebi 458030, P. R. China
tangduo2016@126.com

Jun-Chao Ge

Hebi Institute of Engineering and Technology,
Henan Polytechnic University, Hebi 458030, P. R. China
Faculty of Engineering, Built Environment and Information Technology,
SEGi University, Kota Damansara, Selangor Darul Ehsan 47810, Malaysia
gejunchao@hpu.edu.cn

*Corresponding author: Hui-Na Du
Received January 2, 2024, revised April 21, 2024, accepted August 4, 2024.

Abstract. *The problem of power line loss reduction in an intelligent IoT environment is a very challenging one, but by using IoT technologies and smart algorithms, it is possible to achieve power line loss reduction. High Temperature Superconductor (HTS) plays an important role in the power industry due to its near lossless transmission capability and efficient transmission efficiency. Aiming at the problem that uneven current distribution in each conductive layer of HTS cables will lead to an increase in AC losses, this paper proposes a method for optimising the structural parameters of HTS cables based on a meta-heuristic algorithm. Firstly, the general structure and characteristics of HTS are introduced. Secondly, the AC characteristics of HTS cables are investigated and the AC transmission loss is analysed with emphasis. Then, a function is established with the balanced distribution of currents in each layer as the optimisation objective, and an improved fruit fly optimisation method is used to optimise the structural parameters of the cable's conductive layer. The constraints of the optimisation algorithm are the mechanical characteristics of the HTS cable and the critical current. The experimental results demonstrate the feasibility of the improved FOA algorithm. The structural parameter optimisation of HTS cables using the improved FOA can effectively reduce the AC losses, which can help to realise high-quality transmission and transformation systems over long distances and with high currents.*
Keywords: IoT; Current distribution; FOA; AC losses; Structural parameter optimisation

1. **Introduction.** With the continuous development and application of intelligent Internet of Things (IoT) technology, the smart IoT environment has become an important part of modern society. In the smart IoT environment, various devices, sensors and systems are able to interconnect and form a highly intelligent network. In such an environment, the power system has also gradually realised intelligent management and monitoring. Improving the efficiency of the power system: through the study of power line loss, effective methods can be found to reduce the loss of the power system, thus improving the efficiency and operational stability of the power system.

Meanwhile, with the rapid development of the global economy, the demand for electric energy in social production and life is increasing. Low-loss, high-current and long-distance power transmission is a hot issue in today's society [1, 2, 3, 4]. Due to the nearly lossless power transmission capability as well as efficient transmission efficiency, high-temperature superconductors play an important role in the power industry. Among them, the power loss during AC transmission of high-temperature superconductors is an important research topic.

High temperature superconductor cables are made of HTS materials with almost zero resistance and high current density [5, 6]. When the HTS material is in a superconducting state, the value of the resistance is negligible and the heat loss of the DC current transmitted in the cable is very small. When the HTS cable is transmitting AC power, AC losses will occur. However, as soon as the length of the HTS cable exceeds a certain threshold, the power consumption required to maintain the low temperature state can be partially cancelled out by the AC losses of the cable [7, 8]. At this time, the AC loss of HTS cables will be about 50% lower than the AC loss of normal cables [9]. In practice, it has been found that the transmission capacity of HTS cables is three to five times higher than that of conventional copper cables of the same size. In summary, HTS cables have the advantages of high electrical energy transmission capacity, low heat loss, and small size, and can be used to realise high-capacity, low-loss transmission systems [10, 11].

Nowadays, with the massive migration of population, long-distance transmission of electrical energy is required to meet the increasing consumption of electricity in large cities. However, a large amount of valuable electrical energy is consumed in the cables during transmission. In addition, as electricity consumption continues to grow and the size of the grid continues to increase, the chances of short circuits and other faults continue to increase, seriously affecting the overall power quality. The chances of faults continue to increase, seriously affecting the overall quality of electrical energy. At the same time, short circuits can cause great harm to electrical equipment, and may even lead to the collapse of the power system, resulting in incalculable losses. The use of HTS cables in long-distance power transmission can effectively limit short-circuit currents by utilising the "loss of super" characteristic of HTS, thereby protecting various electrical equipment in the power grid. Superconducting cables can automatically return to the "superconducting state" after the short-circuit current is removed [12]. In addition, the special structure of superconducting cables can make the magnetic field generated by the internal current concentrated in the interior of the cable, preventing the electromagnetic interference of transmission cables from polluting the environment.

Currently, many countries are beginning to plan for the application of superconducting cables to national power grids, thereby achieving an increased level of grid security. With the development of high-temperature superconductor materials, the research of HTS electrical equipment has been paid more and more attention. At this stage, the application of superconducting cables is still in the initial stage. The length requirements of superconducting cables are increasing in various industries [13, 14]. At the same time, the current flow requirement for superconducting cables is also increasing, as shown in Figure 1.

The production process of HTS cables is very different from that of ordinary power cables. Manufacturers need to make superconducting materials that meet the requirements and wind them around the cable skeleton to form HTS cables. The conductive part of HTS cables is usually a multi-layer structure. Each conductive layer consists of a certain number of superconducting materials wound together. Numerous studies have shown [15, 16] that when an alternating current is applied to a cable, the current distribution in each conductive layer is not balanced. Since the amount of current flow in the outer layer is greater than that in the inner layer, the critical current value is reached in the outer layer

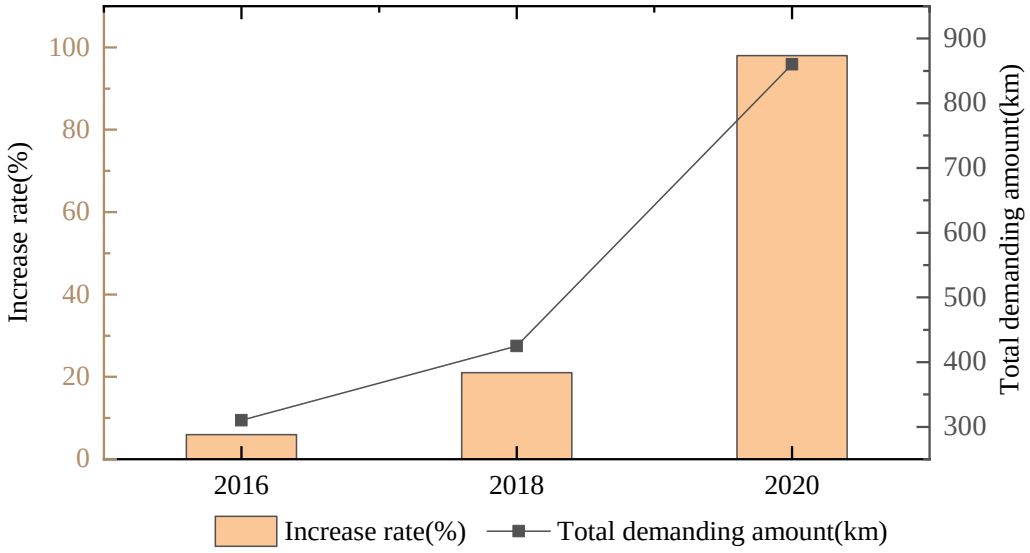

Figure 1. Demand for high-temperature superconductor materials

before the inner layer. This makes the AC loss of the superconducting cable large, which in turn affects the safe and stable operation of the cable [17, 18]. Most of the existing methods for optimising the structural parameters of HTS cables use meta-heuristic algorithms. Optimisation of HTS cable structural parameters using meta-heuristic algorithms can effectively reduce the AC losses, thus helping to achieve high-quality transmission and transformation systems over long distances and with high currents.

1.1. **Related Work.** Meta-heuristic algorithms based on the natural behaviour of animals provide an efficient and simple method for solving complex optimization problems, which has been widely concerned by many scholars. For example, Wang et al. [19] constructed a constrained optimization model for HTS cables with discrete and continuous variables and optimized the structure and other parameters using Particle Swarm Optimization (PSO) algorithm to achieve a balanced distribution of currents among the conductive layers. Liu et al. [20] proposed a robust optimization method for the structure of HTS cables based on six sigma. Compared with the PSO optimisation method, this method not only achieves a uniform current distribution, but also significantly improves the robustness of the HTS cable quality.

Meta-inspired algorithms are intelligent computing algorithms proposed to simulate specific behaviours of nature [21, 22]. With the continuous development of meta-inspired algorithms, various novel meta-inspired algorithms have been proposed one after another [23, 24]. Inspired by the foraging process of fruit flies, Pan Wenchao proposed the Fruit Fly Optimisation Algorithm (FOA) in 2011 [25]. Currently, FOA has been applied in many fields, such as the extreme value problem, the NP-Hard model optimization problem, the optimization problem of generalized regression neural network, the optimization problem of support vector regression, etc. The PSO algorithm needs to regulate five parameters, and has low convergence accuracy; the Artificial Bee Colony (ABC) algorithm needs to regulate four parameters, and is prone to fall into the local optimum; the ant colony algorithm needs to regulate seven parameters, and has complex computation and poor convergence; the genetic algorithm needs to regulate seven parameters, and has complex computation and poor convergence; and the genetic algorithm needs to regulate seven parameters. Bezdan et al. [26] proposed a textual cluster analysis method based on FOA,

and Ibrahim et al. [27] proposed a FOA-based parameter identification method for dual-diode photovoltaic cell models.FOA is simple in principle and requires only 3 parameters to be adjusted, so it is much more efficient than other meta-inspired optimisation algorithms. algorithms, the FOA is more capable of finding the optimum.

Therefore, the aim of this paper is to optimise the structure of HTS cables using the FOA, a meta-heuristic algorithm, so that the currents are uniformly distributed in the various conductive layers, in order to achieve the ultimate effect of reducing AC losses. However, FOA is similar to other algorithms (PSO algorithm and DE algorithm, etc.) in that it is prone to fall into local optimums and has low convergence accuracy. Because FOA has little inter-population variability in the process of selecting generations to find the optimum. Fruit fly has a single learning mode. All fruit fly only gathers to the optimal individual and search for the optimal randomly in its small range. If the optimal fruit fly individual is not the global optimal, FOA can easily fall into the local optimal, resulting in lower convergence accuracy. Aiming at the problems of FOA, there are several improvement schemes. For example, Poluru and Kumar [28] improved the FOA by searching step length, thus dividing the multi-dimensional search space into two parts. Huang et al. [29] introduced a modified local factor into the FOA, thus improving the odour determination rule of fruit fly.

1.2. **Motivation and contribution.** In order to further improve the algorithm's optimisation ability and convergence speed, this paper proposes a novel improved FOA by combining the above two methods. experimental results show that the algorithm's optimisation ability and optimisation efficiency are improved. The main innovations and contributions of this paper include:

(1) Smart meters are used to monitor the current, voltage, power and other parameters of the power lines in real time, and are connected to the IoT system to achieve real-time data collection and transmission. Aiming at the problem that uneven current distribution in each conductive layer of HTS cables will lead to an increase in AC losses, a structural parameter optimisation method for HTS cables based on the Fruit Fly Optimisation Algorithm is proposed under the data-driven approach, so as to make the current in each conductive layer uniformly distributed in order to achieve the ultimate goal of reducing AC losses.

(2) Aiming at the problem that FOA is easy to fall into local optimum and has low convergence accuracy, an improved FOA is proposed. in order to balance the search accuracy and efficiency, this paper adopts a variable step-size strategy and uses the rate of change of odour concentration as a decision criterion to optimize the step-size.

2. Properties of high-temperature superconductors.

2.1. **Basic structure of HTS.** Superconductors have good ductility and uniform grain distribution. The material densification of superconductors can be promoted by heat treatment, which can repair the cracks that will be produced in deformation processing [30]. Therefore, by heat treatment, superconductors can improve the inter-grain connectivity and facilitate the processing into cables. High-temperature superconductor power technology can improve the inherent drawbacks of conventional power technology and will bring about a major change in the power transmission system. Based on the special electrical properties of superconductors, the application of superconductor technology will greatly improve the stability and intelligence of power transmission systems.

HTS will surely become the key to establish smart grid and play a decisive role. The basic structure of HTS cable is shown in Figure 2.

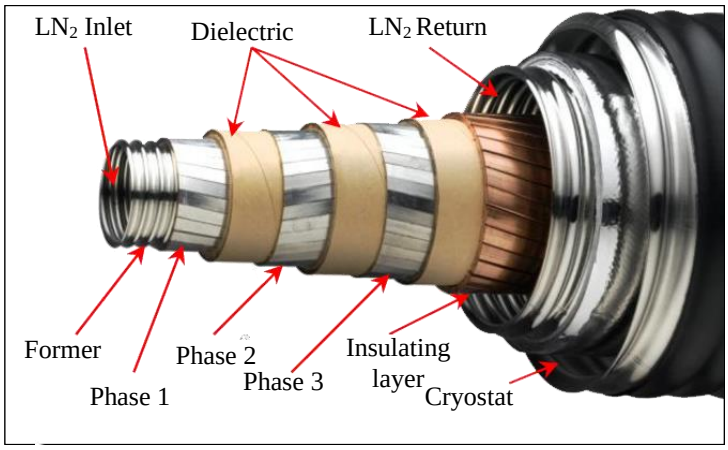

Figure 2. Basic structure of HTS cables

It can be seen that the high temperature superconducting cable is structurally symmetrical in the axial direction and has a relatively uniform material distribution. When operating at rated current, the temperature of the HTS is typically that of liquid nitrogen, i.e. 77 K. It is generally assumed that the steady state temperature of the HTS does not change in the axial direction and that there is good contact between the objects, so that the contact thermal resistance of the HTS can be approximated and ignored. Inside the insulating layer, Phase 1, Phase 2 and Phase 3 are the strips of HTS.

2.2. **Basic properties of HTS.** A large number of experiments show that superconductors have three major properties: zero resistance, Meissner effect (completely antimagnetic), and Josephson effect. Zero resistance effect is the basis for having lossless current transmission. At low temperatures, metals in general have a certain resistance, and there is a certain relationship between their resistivity and temperature [**?**].

$$\rho = \rho_0 + AT^5 \tag{1}$$

where ρ_0 is the resistance at $T = 0$ K, also known as the residual resistance. The magnitude of the residual resistance is related to the purity of the metal and the integrity of the material lattice. The metal material will always have impurities and workmanship defects, so metal cable will definitely have a residual resistance.

In 1911, the Dutch scientist Onnes was surprised to find that the resistance of mercury was almost zero near 4.2 K. When the temperature reached a critical level, the resistance suddenly dropped to zero. When the temperature reaches a critical value where the resistance suddenly falls to zero, this is the phenomenon of no resistance, also known as superconductivity. The size of the temperature at which the resistance of a superconductor falls sharply to zero is called the critical temperature of superconductivity, and is expressed as T_C. The resistance versus temperature curve of a high-temperature superconductor is shown in Figure 3. $T_{C,\text{onset}}$ indicates the starting transition temperature, and T_{C0} the temperature at which the resistance has just dropped to zero (zero resistance temperature).

Superconductors have both zero resistance (full electrical conductivity) and the Meissner effect (full antimagnetism), which are two of the most fundamental properties of superconductors. They are both independent and closely related. The Meissner effect can be demonstrated by a magnetic levitation experiment, in which a permanent magnet is slowly dropped towards a superconductor, and the magnet is suspended at a certain height without touching the superconductor. The basic principle is the same as that of

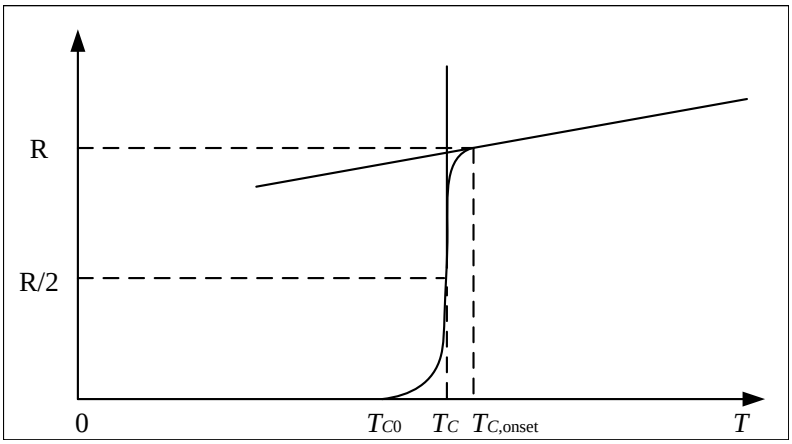

Figure 3. Resistance and Temperature Characteristics of HTS

a maglev train, i.e. the lines of magnetic induction from the permanent magnet cannot pass through the superconductor. The magnetic field's lines of magnetic induction are distorted, creating an upward repulsive force. The repulsive force is balanced by the magnet's gravitational force, and the magnet levitates above the superconductor.

Inside the superconductor, the flux density generated by the shielding current at the surface of the superconductor cancels out the flux density induced by the external field, so that the net flux density of the superconductor is zero, as shown in Figure 4.

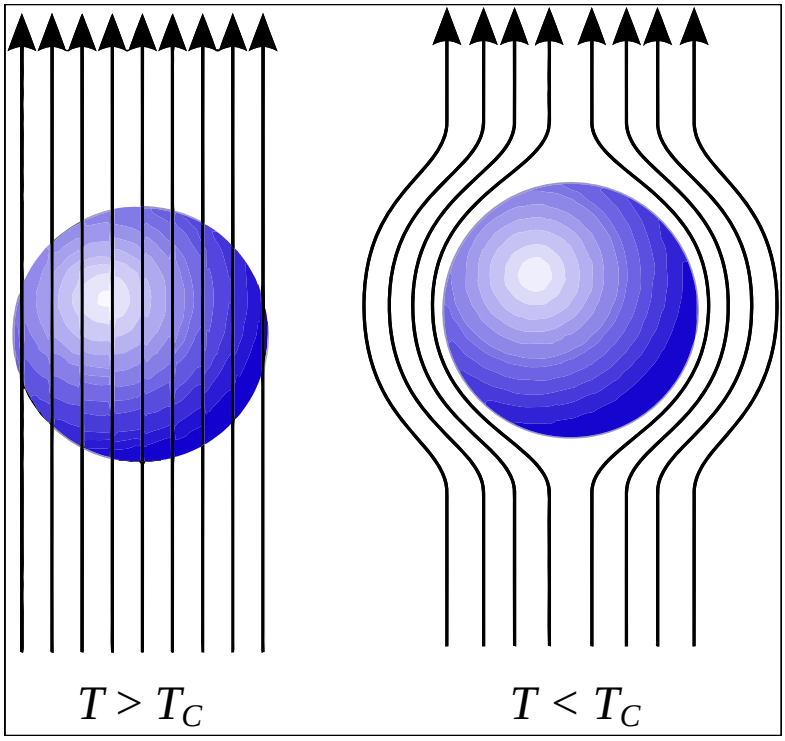

Figure 4. Meissner effect

The Josephson effect is a microscopic quantum effect. If a very thin insulating layer is added between two superconductors, a weak connection between the two superconductors occurs, resulting in a tunneling current, as shown in Figure 5. When the current is greater than a critical value, Andreev reflection occurs at the Josephson junction. When

the voltage difference between the two superconductors exceeds the bandgap voltage, the Andreev reflection on the Josephson junction disappears.

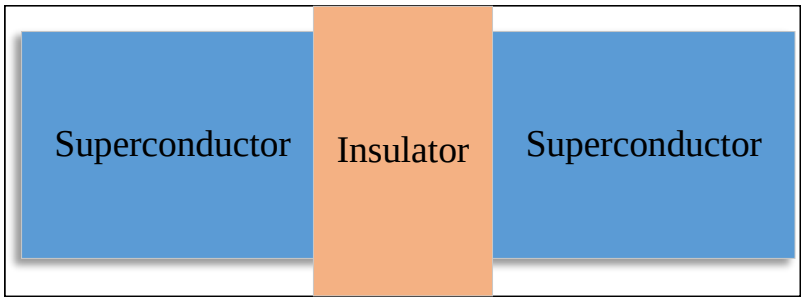

Figure 5. The Josephson Effect Knot

The above three features make HTS cables have the advantages of low loss, large capacity and compact structure in practical application. In addition, superconductors can effectively reduce stray electric and magnetic fields, thus preventing electromagnetic pollution.HTS cables can withstand large short-circuit currents in a short period of time and allow a long overload time. After the short circuit is over, HTS cables can recover by themselves. Therefore, HTS cables can greatly improve the stability and intelligence of the power grid system.

3. **AC characteristics of HTS cables.** HTS cables will have losses within the superconductor whenever they transmit AC power. AC losses are due to the induced electric field in the superconductor by the changing magnetic field when the superconductor is energised with alternating current or electromagnetic perturbation [32]. According to Faraday's law of electromagnetism, when a superconductor is in an alternating magnetic field, the magnetic induction strength through the conductor changes as the magnetic field changes. The changing magnetic field will generate an induced electromotive force in the conductor, which produces an electric field of a certain strength E. With the generation of the induced electric field, an induced current will also be generated, and the product of the induced current density J and the electric field E is the loss power per unit volume $J \cdot E$. Integration of the loss power $J \cdot E$ per unit volume of an HTS cable gives the AC loss P.

$$P = \int_0^T dt \int J \cdot E d^3 r \tag{2}$$

From Poynting's theorem, we obtain Equation (3).

$$J \cdot E = \frac{\partial w}{\partial t} + \nabla \cdot S \tag{3}$$

where $S = E \times H$ is the Poynting vector and w is the energy density. Using the scattering theorem and Maxwell's equation, we can transform Equation (2).

$$P = \int_0^T dt \int J \cdot E dV + \int_0^T dt \int H \cdot \frac{\partial M}{\partial t} dV \tag{4}$$

where M is the magnetisation intensity and J is the Maxwell current density. The schematic diagram of the conductive layer of the HTS cable is shown in Figure 6.

The radius of the conductive layer is R, the winding angle is β, the width of the strip is w, the axial distance between neighbouring strips is d, and the pitch of the individual strip is L.

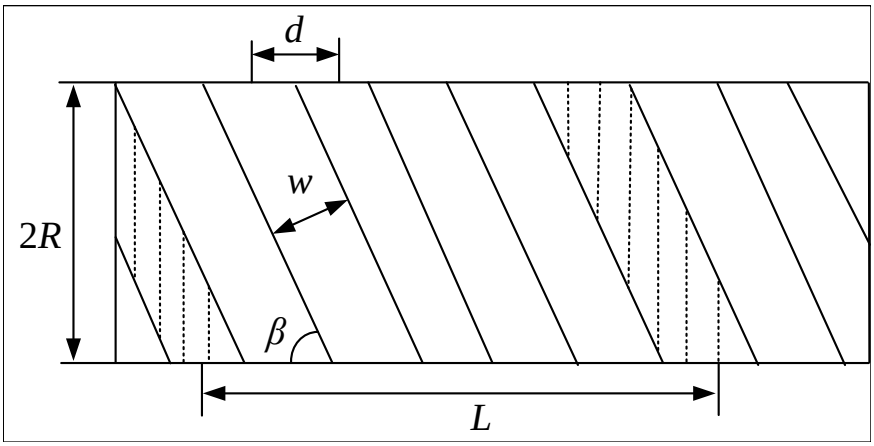

Figure 6. Schematic representation of the conductive layer of the HTS cable

$$\tan\beta = \frac{2\pi R}{L} \tag{5}$$

$$d = \frac{w}{\sin\beta} \tag{6}$$

In HTS cables, both the shielding layer and the conductive layer are made of superconducting cables wound in a certain direction. The winding direction of each layer is not necessarily the same. Therefore, when passing through the AC current, the conductive layer of the HTS cable will have resistance, self-inductance and interlayer mutual inductance, while the shield layer will also have resistance, self-inductance and interlayer mutual inductance, and there is also mutual inductance between the conductive layer and the shield layer. At the same time, mutual inductance exists between the conductive layer and the shielding layer. The equivalent circuit of the HTS cable is shown in Figure 7.

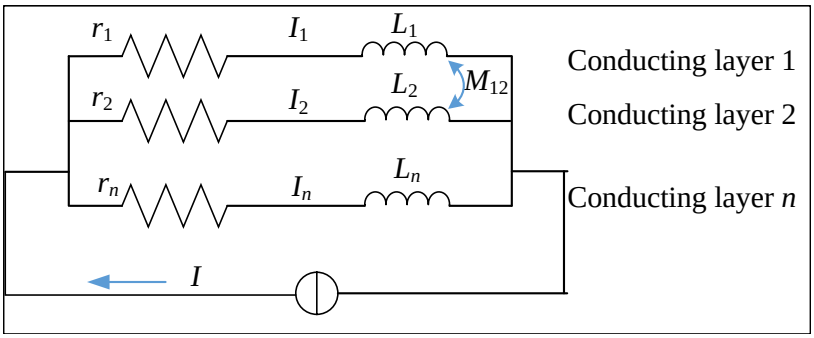

Figure 7. Equivalent circuit of HTS cable

Currently, there are three commonly used methods for measuring the AC loss of superconducting materials: the magnetic, electrical, and thermal methods. The AC magnetisation method is a commonly used calculation method in the characterisation of AC losses in conventional magnetic materials. The superconducting loss can be calculated based on the magnitude of the superconducting AC magnetisation.

$$P = \frac{Sf\pi B_m^2}{\mu_0}\mu' \tag{7}$$

where μ' is the imaginary part of the AC magnetisation of the superconductor, μ_0 is the vacuum permeability, B_m the alternating magnetic field amplitude, f is the frequency of the alternating magnetic field, and S is the effective cross-sectional area of the superconductor.

4. **Optimisation of structural parameters of HTS cable based on improved FOA in IoT environment.**

4.1. **FOA algorithm.** The FOA is a new approach to global optimisation that has been widely used in science and engineering. Currently, the FOA has been successfully applied to solve mathematical function extremes, support vector machine parameter optimisation and neural network model parameter optimisation [33]. The principle of fruit fly population searching for food is shown in Figure 8.

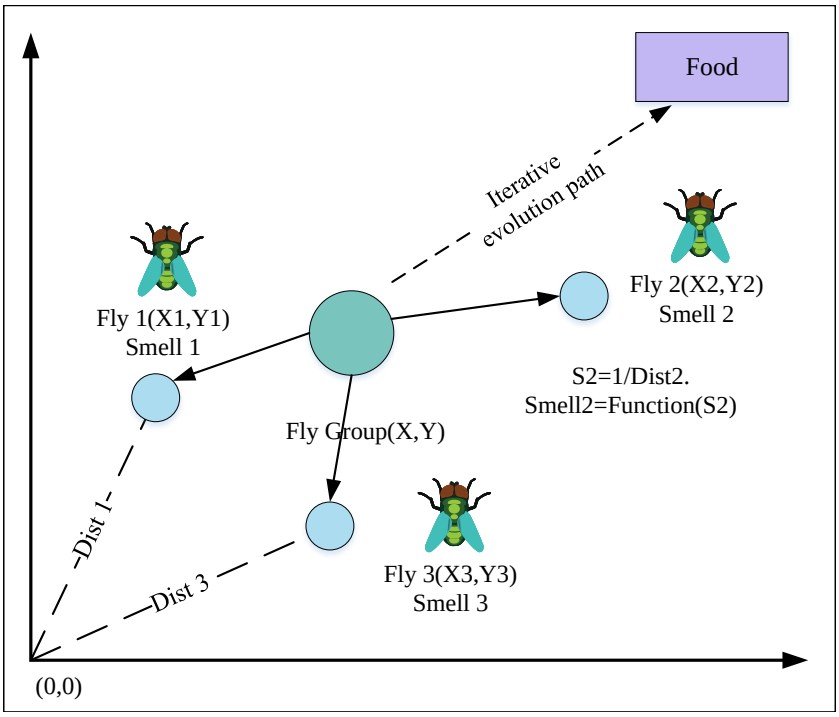

Figure 8. Principles of food searching in fruit fly groups

The initial positions of the FOA are X_{init} and Y_{init}. All the fruit fly individuals in the FOA move randomly in any direction position and thus position updates occur continuously.

$$X_i = X_{\text{init}} + H_r \tag{8}$$

$$Y_i = Y_{\text{init}} + H_r \tag{9}$$

where H_r is a random number with values in the range $[-H, H]$.

$$H_r = H \times [2 \times \text{rand}() - 1] \tag{10}$$

where H is the maximum step size [34].

The distance of an individual fruit fly from the origin is d.

$$d = \sqrt{X_i^2 + Y_i^2} \tag{11}$$

$$S_i = 1/d \tag{12}$$

where S_i is the flavour concentration determination value. In this paper, S_i is used as a variable to solve for flavour concentration.

$$\text{Smell}_i = \text{Function}(S_i) \tag{13}$$

where *Function* is the fitness function. Firstly, the optimal value is output as bestSmell_i, and the coordinates corresponding to the optimal value are $(X_{\text{best}}, Y_{\text{best}})$. Next, take the coordinates of the optimal value as the new coordinates of the current fruit fly swarm, and repeat the process execution of Equation (8) to Equation (13). Compare the current optimal value with the optimal value of the last iteration until the maximum number of iterations is reached.

4.2. **Improved FOA.** In the optimisation process, the search step size has a more obvious impact on the performance of FOA [35]. In order to balance the search accuracy and efficiency, this paper adopts a variable step size strategy. A larger step size in the early stage is used to quickly find a more optimal solution, and a smaller step size is used to find the global optimal solution in the later stage. The variable step size strategy can effectively reduce the probability of local optimum of FOA, thus improving the convergence accuracy.

In order to improve the convergence speed of the variable step-size strategy, this paper combines the adaptive step-size and odour determination rule. In this paper, the rate of change of flavour concentration is used as the decision criterion for step length optimization, thus improving both the optimality searching ability and the optimality searching efficiency. Let the rate of change of flavour concentration be R.

$$R = \frac{|\min(\text{Smell}_i) - \max(\text{Smell}_i)|}{|\min(\text{Smell}_{i-1}) - \max(\text{Smell}_{i-1})| + \delta} \tag{14}$$

where δ is a tiny constant to prevent a denominator of 0 and Smell_i is the value of odour concentration after the i-th iteration.

Different step sizes are taken depending on the R value. When R is large, it indicates that the odour concentration of the FOA is more variable and a larger search step should be taken. The step size of the i-th iteration H_i in relation to the previous iteration is shown below.

$$H_i = H_{i-1} + \tan\left(\left(1 - \frac{g}{\text{Maxgen}}\right) * 3\right) * H_{i-1} \tag{15}$$

When $R \in [R_{\min}, R_{\max}]$ indicates a small change in the concentration value, this is when the step size should be reduced to find the optimal solution.

$$H_i = H_{i-1} - \tan\left(\frac{g}{\text{Maxgen}} * 5\right) * H_{i-1} \tag{16}$$

The specific steps to improve the FOA are shown below: (1) Set both the number of fruit fly populations and the number of iterations to 100. The initialisation position of the fruit fly population is randomly distributed in the range of [0,2], and the flight range is [-10,10].

(2) Initialise the fitness function, the optimal position $(X_{\text{best}}, Y_{\text{best}})$ and the individual fruit fly flight range.

(3) Calculate the flavour concentration value S.

$$S_i = \frac{1}{\text{Dist}_i} \tag{17}$$

where Dist_i denotes the distance from the individual's coordinate point to the origin of the coordinate system, i.e., $\text{Dist}_i = \sqrt{x_i^2 + y_i^2}$.

(4) The root mean square error is used to construct the adaptivity function D_i in order to determine the flavour concentration value S, i.e. $D_i = F(S_i)$.

(5) Seek the initial extreme value according to the adaptivity function, i.e. find the position of the individual fruit fly with the highest flavour concentration.

(6) Compare the current best flavour concentration with the best flavour concentration of the previous generation, if the former is greater than the latter, skip to Step 7. If the former is greater than the latter, skip to Step 7. If the former is greater than the latter, then skip to Step 7, otherwise skip to Step 3. save the value of the best flavour concentration and the corresponding coordinates.

Step 7: Determine whether the maximum number of iterations has been reached. If yes, the current optimal flavour concentration value is the optimal Function parameter.

4.3. **Optimisation Objective Function Driven by IoT Data.** In this work, smart meters can be used to monitor the power consumption of power lines, and smart meters can achieve remote data collection and transmission to provide data support for power line loss research. The smart meter is the core device of the electric power intelligent IoT system, which can realise the comprehensive monitoring and data collection of the power line loss and provide sufficient data support for the power line loss research.

The smart meter mainly collects and acquires power quality parameters such as voltage, current and power factor. In addition, the temperature data of the cable line, including the surface temperature and the internal temperature of the cable line, are also collected by devices such as temperature sensors. High temperature is an important factor that affects the AC loss of cable lines. By collecting this data, power usage can be analysed to optimise power usage and reduce power line losses. Numerous studies have shown that uniform current distribution between layers and uniform distribution of electromagnetic fields are the main objectives of the optimal design of HTS cables. When HTS cables are energised with alternating currents, the current distribution in each layer is unbalanced. The current distribution in the outer layer is significantly more than that in the inner layer during operation. As a result, when the total current gradually increases, the current flowing in the outer layer reaches the current threshold before the inner layer. This uneven current distribution will make the AC loss of the HTS cable large, thus affecting the safe and stable operation of the cable. According to the equivalent circuit of HTS cable, we can derive the current matrix.

$$\begin{bmatrix} I_1 \\ \vdots \\ I_m \\ I_{m+1} \\ \vdots \\ I_{m+n} \end{bmatrix} = \frac{1}{j\omega} \begin{bmatrix} L_1 & \dots & M_{1,n} & M_{1,n+1} & \dots & M_{1,m+n} \\ \vdots & \ddots & \vdots & \vdots & \ddots & \vdots \\ M_{m,1} & \dots & L_m & M_{m,n+1} & \dots & M_{m,m+n} \\ M_{m+1,1} & \dots & M_{m+1,m} & L_{m+1} & \dots & M_{m+1,m+n} \\ \vdots & \ddots & \vdots & \vdots & \ddots & \vdots \\ M_{m+n,1} & \dots & M_{m+n,m} & M_{m+n,m+1} & \dots & L_{m+n} \end{bmatrix}^{-1} \begin{bmatrix} U \\ \vdots \\ U \\ 0 \\ \vdots \\ 0 \end{bmatrix} \tag{18}$$

where L_i is the self-inductance of layer i and M_{ij} is the mutual inductance between layers i and j. The magnitude of the current in each layer of the HTS cable is related to the above two parameters.

$$L_i = \mu_0 \left(\frac{\pi r_i^2}{P_i^2} + \frac{1}{2\pi} \ln \frac{R}{r_i} \right) = \frac{\mu_0}{4\pi} \left(\tan^2 \beta_i + 2 \ln \frac{R}{r_j} \right) \tag{19}$$

$$M_{ij} = M_{ji} = \mu_0 \left(\frac{\alpha_i \alpha_j}{P_i P_j} \frac{\pi r_i^2}{r_j} + \frac{\mu_0}{2\pi} \ln \frac{R}{r_j} = \frac{\mu_0}{2\pi} \left(\frac{\alpha_j r_i}{2} \tan \beta_i + \ln \frac{R}{r_j} \right) \right) \tag{20}$$

where r is the equivalent resistance. It can be seen that the magnitude of self-inductance and mutual inductance depends on the winding direction α, the winding angle β, and the radius of superconducting material in each layer R. For Z-type HTS cables, $\alpha = 1$. For S-type HTS cables, $\alpha = -1$. By varying the magnitude of α, β and R, the self-inductance and mutual inductance of the various layers of the HTS cables can be varied, and thus the current distribution of the various layers can be varied. If the current distribution in each layer is uniform, the AC loss reduction effect can be achieved. Therefore, the optimal design of HTS cables can be optimised at each layer for the three parameters α, β and R.

The optimisation objective function in this paper is set as $Function(x) = min(f(x))$.

$$minf(X) = \sum_{i=1}^{n-1} \sum_{j=i+1}^{n} |I_{x_i}(X) - I_{x_j}(X)| + \sum_{i=1}^{n-1} \sum_{j=i+1}^{n+1} |I_{y_i}(X) - I_{y_j}(X)| \tag{21}$$

where I_{x_i} and I_{y_i} are the real and imaginary parts of the AC vector X in layer i, respectively. The vector $X = [\beta, \alpha, R, \beta_2, \alpha_2, R_2, \cdots, \beta_n, \alpha_n, R_n]$ consists of structural parameters such as winding angle β, winding direction α and radius R of each layer of the strip.

Conditional constraints need to take into account the radius, winding angle and winding direction, and also the critical current of the superconductor. The magnitude of the optimised current must be less than its critical current to ensure that the superconductor is in a superconducting state. The parameter X when $f(x)$ is taken to its minimum value is the optimal structural parameter of the HTS cable, subject to the given constraints.

5. **Experimental Results and Analyses.**

5.1. **Performance Validation of Improved FOA.**

In order to test the optimisation finding ability of the improved FOA, seven classical functions were used as the fitness functions for the experiments.

The dimensions of the seven classical functions are all 30. The meta-heuristic algorithms such as FOA, IMFOA [36], MFOA [37], PSO [38], and DE [39] are compared with the improved FOA proposed in this paper under the same conditions. The correlation properties of the seven classical functions are given in Table 1, where $f_1 - f_4$ is a single-peak function (with only one extreme point) and $f_5 - f_7$ is a multi-peak function (with more than two extreme points). The single-peak function is used to test the algorithm's speed of generation selection and ability to find local optima, while the multi-peak function is used to test the algorithm's convergence accuracy and ability to find global optima. For a fair comparison of these six meta-inspired algorithms, the cluster size was set to 20 and the maximum number of iterations was 500 for all of them. The upper limit R_{max} and lower limit R_{min} of the rate of change of concentration in the improved FOA were 1.0. Each algorithm was run independently for 20 times and averaged in the end.

$$f_1(x) = \sum_{i=1}^{n} x_i^2 \tag{22}$$

$$f_2(x) = \sum_{i=1}^{n} |x_i| + \prod_{i=1}^{n} |x_i| \tag{23}$$

$$f_3(x) = \sum_{i=1}^{n} \left(\sum_{j=1}^{i} x_j \right)^2 \tag{24}$$

$$f_4(x) = \sum_{i=1}^{n} \left[100 \left(x_{i+1} - x_i^2 \right)^2 + (1 - x_i)^2 \right] \tag{25}$$

$$f_5(x) = \sum_{i=1}^{n} \left(x_i^2 - 10 \cos(2\pi x_i) + 10 \right) \tag{26}$$

$$f_6(x) = \frac{1}{4000} \sum_{i=1}^{n} x_i^2 - \prod_{i=1}^{n} \cos\left(\frac{x_i}{\sqrt{i}} \right) + 1 \tag{27}$$

$$f_7(x) = \sum_{i=1}^{n} x_i \sin(x_i) + 0.1 x_i \tag{28}$$

Table 1. Test function

Function name	**Scope of the search for excellence**	**Optimum value**	**Target accuracy**
Sphere	[-100,100]	0	10^{-13}
Schwefel 2.22	[-10,10]	0	10^{-5}
Schwefel 1.2	[-100,100]	0	10^{-10}
Rosenbrock	[-30,30]	0	10^{-2}
Rastrigin	[-5.12,5.12]	0	10^{-10}
Griewank	[-600,600]	0	10^{-15}
Alpine	[-10,10]	0	10^{-6}

The test results of the seven fitness functions for the four FOAs are listed in Table 2. Mean denotes the average optimised value and Std denotes the average standard deviation. It can be seen that the average optimised value and the average standard deviation of the improved FOA proposed in this paper are better than those of FOA, IMFOA and MFOA, regardless of whether it is a single-peak function or a multi-peak function.

Table 2. Test Results for 4 FOAs

	Ours		**FOA**		**IMFOA**		**MFOA**	
	Mean	**Std**	**Mean**	**Std**	**Mean**	**Std**	**Mean**	**Std**
f_1	2.52E-39	1.57E-39	2.35E-04	1.75E-06	3.47E-15	8.16E-18	3.51E-05	2.32E-05
f_2	2.56E-19	7.09E-20	8.39E-02	2.36E-04	3.22E-07	4.65E-10	8.53E-04	2.19E-05
f_3	2.77E-38	9.63E-39	3.60E-03	3.50E-05	5.22E-14	1.89E-16	5.02E-04	2.66E-04
f_4	8.24E-21	1.44E-21	2.90E-03	2.13E-05	1.17E-08	4.79E-11	7.67E-04	2.57E-05
f_5	2.40E+01	2.57E-03	2.87E+01	7.30E-05	2.90E+01	1.58E-04	2.87E+01	3.92E-02
f_6	6.10E-05	7.13E-05	2.80E-03	6.13E-04	9.49E-05	9.18E-05	1.12E-03	8.21E-04
f_7	-1.00E+00	0.00E+00	-9.96E-01	3.12E-08	-1.00E+00	7.40E-17	-1.00E+00	1.62E-04

Table 3 lists the experimental results of the proposed improved FOA in comparison with PSO and DE. It can be seen that the mean and average standard deviation are better than PSO and DE in the results of the improved FOA proposed in this paper for solving the seven test functions.

The average number of convergence of the proposed improved FOA to reach the target accuracy is less than the other algorithms for a given target accuracy. In addition, FOA has a success rate of 0 in achieving the target accuracy for all functions. Overall, the proposed improved FOA outperforms the other five algorithms.

Table 3. Test results of different metaheuristic algorithms

	Ours		**PSO**		**DE**	
	Mean	**Std**	**Mean**	**Std**	**Mean**	**Std**
f_1	2.52E-39	1.57E-39	1.42E+00	4.70E-01	8.97E+03	3.30E+03
f_2	2.56E-19	7.09E-20	4.94E+00	8.90E-01	2.21E+00	5.49E+00
f_3	2.77E-38	9.63E-39	1.64E+01	5.41E+00	1.02E+05	5.11E+04
f_4	8.24E-21	1.44E-21	4.93E-01	7.89E-02	3.29E+01	3.05E+00
f_5	2.40E+01	2.57E-03	1.51E+02	2.91E+01	7.65E+02	1.57E+03
f_6	6.10E-05	7.13E-05	2.85E+00	1.66E-01	2.05E-02	6.24E-03
f_7	-1.00E+00	0.00E+00	-3.57E-02	1.73E-02	0.00E+00	0.00E+00

5.2. **Example of HTS cable optimisation.** The proposed improved FOA is used to optimise the structural parameters of the HTS cable produced by Zhongtian Technology Company as an example.The rated operating voltage of the HTS cable is 110 kV, the length is 1 km, and the peak current is 3 kA.The structural parameters of the HTS cable are shown in Table 4. The model of the smart meter is Acrel ADL300-E, the communication interface is RS485, the measurement error of active energy is less than $\pm 0.5\%$, and the current range is 5A to 100A.

Table 4. Structural parameters of HTS cables

Number	α	$\beta(^\circ)$	R **(mm)**
1	+1	25	13.25
2	-1	25	13.50
3	+1	25	13.75
4	-1	25	14.00
5	-1	25	28.00
6	+1	25	28.25

The calculated current waveforms are shown in Figure 9 when an alternating current with a peak value of 2 kA is passed through the HTS cable. It can be seen that the currents in each layer have large differences in amplitude and phase. The outer layer current is obviously larger than the inner layer current. The current value of layer 4 competes to reach about 10 times of layer 1, while the current of layer 2 is reversed with other currents.

Next, the structural parameters of the HTS cable are optimised using the improved FOA proposed in this paper. The objective function is Equation (21). The constraints are:

$$R \in [12.25\text{mm}, 13.25\text{mm}], \quad \beta \in [12^\circ, 37^\circ], \quad \alpha = \pm 1 \tag{29}$$

Changing the matrix of each structural parameter, the structural parameters of the optimised HTS cable are shown in Table 5. It can be seen that the current distribution in each conductive layer is basically balanced after parameter optimisation. When a current with a peak value of 2 kA is passed through the optimised cable, the waveforms of the currents in each conductive layer are shown in Figure 10. It can be seen that the currents in each layer converge in amplitude and phase.

The AC losses in the conductive layer of the HTS cable before and after optimisation are calculated separately at different current strengths and the results are shown in Figure 11. It can be seen that with the increase of current, the AC loss of the cable conductive layer grows. However, the AC loss after optimisation is significantly smaller

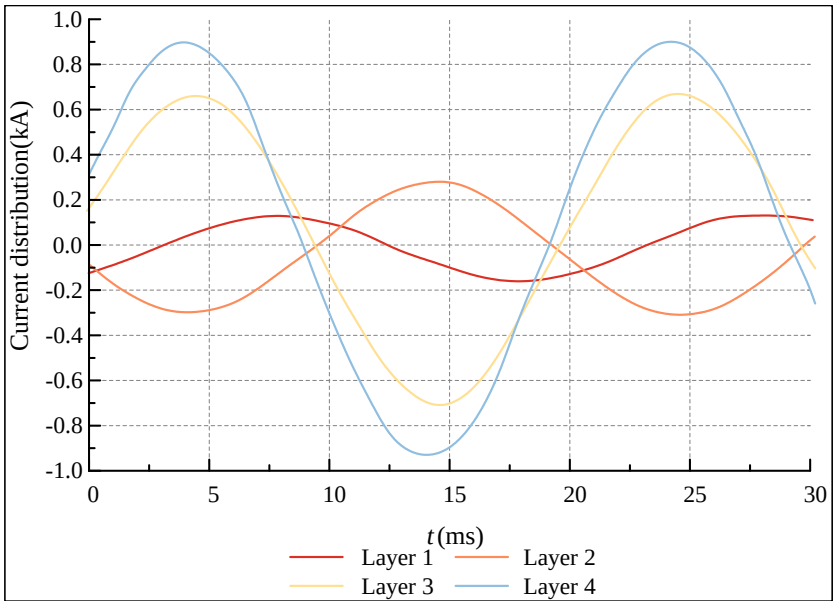

Figure 9. Current distribution in layers before optimisation

Table 5. Structural parameters of the optimised HTS cable

Number	$\boldsymbol{\alpha}$	$\boldsymbol{\beta}(^\circ)$	$\boldsymbol{R}$**(mm)**
1	+1	28.5	13.25
2	+1	13.4	13.51
3	-1	12.3	13.75
4	-1	36.3	14.12
5	+1	19.5	27.95
6	-1	19.6	28.22

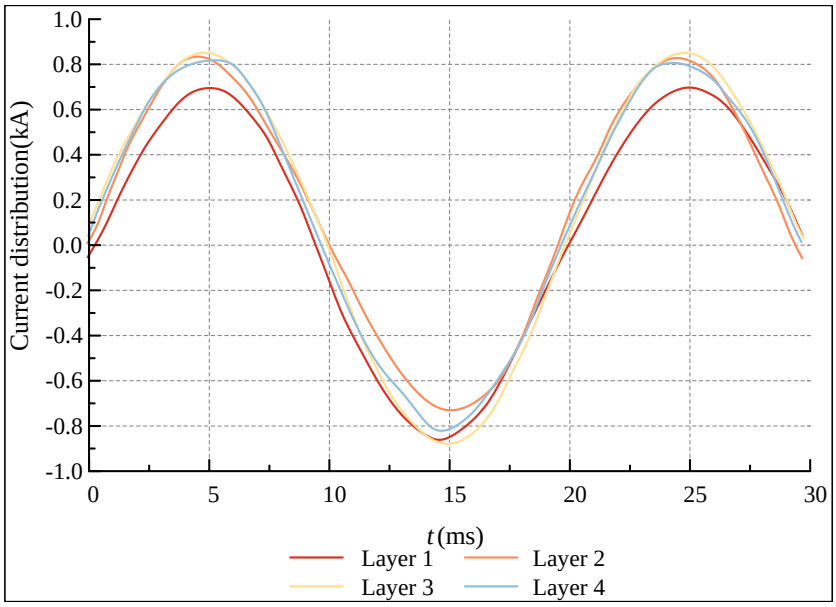

Figure 10. Optimised current distribution in layers

than that before optimisation, which indicates that making the current in each conductive layer uniformly distributed can reduce the AC loss of the HTS cable during operation.

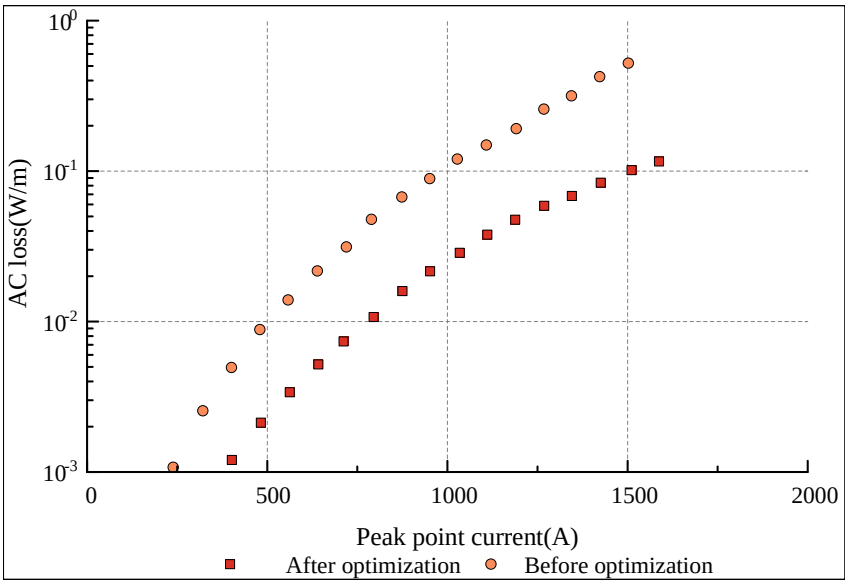

Figure 11. AC losses in the conductive layer of HTS cables before and after optimisation

6. **Conclusion.** HTS plays an important role in the power industry due to its near lossless transmission capability and high transmission efficiency. Among them, the power loss during HTS AC transmission is an important research topic. In order to solve the problem of power line loss reduction in the smart IoT environment, a method for optimising the structural parameters of HTS cables based on the Fruit Fly Optimisation Algorithm (FOA) is proposed, which leads to a uniform distribution of the current in the various conductive layers in order to achieve the ultimate goal of reducing the AC loss. In order to solve the problems of FOA easily falling into local optimum and low convergence accuracy, a variable step size strategy is adopted to propose an improved FOA, and the rate of change of flavour concentration is used as a decision criterion for step size optimisation. Adjusting the parameters such as winding angle, winding direction and radius of the conductive layer of HTS cables are the main factors for the current equalisation between layers. Therefore, adjusting these three parameters means that the HTS cable can be optimised. The experimental results demonstrate the feasibility of the improved FOA. The optimisation of structural parameters of HTS cables using the improved FOA can effectively reduce the AC losses, which can help to realise high-quality transmission and transformation systems over long distances and with high currents.

REFERENCES

[1] J. A. Flores-Livas, L. Boeri, A. Sanna, G. Profeta, R. Arita, and M. Eremets, "A perspective on conventional high-temperature superconductors at high pressure: Methods and materials," *Physics Reports*, vol. 856, pp. 1-78, 2020.

[2] B. Shen, F. Grilli, and T. Coombs, "Overview of *H*-Formulation: A Versatile Tool for Modeling Electromagnetics in High-Temperature Superconductor Applications," *IEEE Access*, vol. 8, pp. 100403-100414, 2020.

[3] S. Hahn, K. Kim, K. Kim, X. Hu, T. Painter, I. Dixon, S. Kim, K. R. Bhattarai, S. Noguchi, J. Jaroszynski, and D. C. Larbalestier, "45.5-tesla direct-current magnetic field generated with a high-temperature superconducting magnet," *Nature*, vol. 570, no. 7762, pp. 496-499, 2019.

[4] S. C. Wimbush, and N. M. Strickland, "A Public Database of High-Temperature Superconductor Critical Current Data," *IEEE Transactions on Applied Superconductivity*, vol. 27, no. 4, pp. 1-5, 2017.

[5] B. Keimer, S. A. Kivelson, M. R. Norman, S. Uchida, and J. Zaanen, "From quantum matter to high-temperature superconductivity in copper oxides," *Nature*, vol. 518, no. 7538, pp. 179-186, 2015.
[6] W.-K. Kwok, U. Welp, A. Glatz, A. E. Koshelev, K. J. Kihlstrom, and G. W. Crabtree, "Vortices in high-performance high-temperature superconductors," *Reports on Progress in Physics*, vol. 79, no. 11, 116501, 2016.
[7] H. H. Kim, S. M. Souliou, M. E. Barber, E. Lefrançois, M. Minola, M. Tortora, R. Heid, N. Nandi, R. A. Borzi, G. Garbarino, A. Bosak, J. Porras, T. Loew, M. König, P. J. W. Moll, A. P. Mackenzie, B. Keimer, C. W. Hicks, and M. Le Tacon, "Uniaxial pressure control of competing orders in a high-temperature superconductor," *Science*, vol. 362, no. 6418, pp. 1040-1044, 2018.
[8] Y. Zhao, J. M. Zhu, G. Y. Jiang, C. S. Chen, W. Wu, Z. W. Zhang, S. K. Chen, Y. M. Hong, Z. Y. Hong, Z. J. Jin, and Y. Yamada, "Progress in fabrication of second generation high temperature superconducting tape at Shanghai Superconductor Technology," *Superconductor Science and Technology*, vol. 32, no. 4, 044004, 2019.
[9] X. Feng, J. Zhang, G. Gao, H. Liu, and H. Wang, "Compressed sodalite-like MgH_6 as a potential high-temperature superconductor," *RSC Advances*, vol. 5, no. 73, pp. 59292-59296, 2015.
[10] B. Meredig, E. Antono, C. Church, M. Hutchinson, J. Ling, S. Paradiso, B. Blaiszik, I. Foster, B. Gibbons, J. Hattrick-Simpers, A. Mehta, and L. Ward, "Can machine learning identify the next high-temperature superconductor? Examining extrapolation performance for materials discovery," *Molecular Systems Design & Engineering*, vol. 3, no. 5, pp. 819-825, 2018.
[11] S. Dadras, S. Dehghani, M. Davoudiniya, and S. Falahati, "Improving superconducting properties of YBCO high temperature superconductor by Graphene Oxide doping," *Materials Chemistry and Physics*, vol. 193, pp. 496-500, 2017.
[12] E. Zurek, and T. Bi, "High-temperature superconductivity in alkaline and rare earth polyhydrides at high pressure: A theoretical perspective," *The Journal of Chemical Physics*, vol. 150, no. 5, 45-53, 2019.
[13] C. Lee, H. Son, Y. Won, Y. Kim, C. Ryu, M. Park, and M. Iwakuma, "Progress of the first commercial project of high-temperature superconducting cables by KEPCO in Korea," *Superconductor Science and Technology*, vol. 33, no. 4, 044006, 2020.
[14] A. Augieri, G. De Marzi, G. Celentano, L. Muzzi, G. Tomassetti, F. Rizzo, A. Anemona, A. Bragagni, M. Seri, C. Bayer, N. Bagrets, and A. della Corte, "Electrical Characterization of ENEA High Temperature Superconducting Cable," *IEEE Transactions on Applied Superconductivity*, vol. 25, no. 3, pp. 1-4, 2015.
[15] W. Xie, B. Wei, and Z. Yao, "Introduction of 35 kV km Level Domestic Second Generation High Temperature Superconducting Power Cable Project in Shanghai, China," *Journal of Superconductivity and Novel Magnetism*, vol. 33, no. 7, pp. 1927-1931, 2020.
[16] A. Zappatore, A. Augieri, R. Bonifetto, G. Celentano, L. Savoldi, A. Vannozzi, and R. Zanino, "Modeling quench propagation in the ENEA HTS cable-in-conduit conductor," *IEEE Transactions on Applied Superconductivity*, vol. 30, no. 8, pp. 1-7, 2020.
[17] O. Rahman, K. M. Muttaqi, and D. Sutanto, "High Temperature Superconducting Devices and Renewable Energy Resources in Future Power Grids: A Case Study," *IEEE Transactions on Applied Superconductivity*, vol. 29, no. 2, pp. 1-4, 2019.
[18] R. K. Gadekula, and R. S. Dondapati, "Entropy Generation Minimization (EGM) in High Temperature Superconducting (HTS) cables for optimization of thermohydraulic performance," *Physica C: Superconductivity and its Applications*, vol. 566, 1353541, 2019.
[19] X. Liu, S. Wang, J. Qiu, J. G. Zhu, Y. Guo, and Z. W. Lin, "Robust optimization in HTS cable based on design for six sigma," *IEEE Transactions on Magnetics*, vol. 44, no. 6, pp. 978-981, 2008.
[20] L. Xinying, W. Shuhong, Q. Jie, Z. Jian Guo, G. Youguang, and L. Zhi Wei, "Robust Optimization in HTS Cable Based on Design for Six Sigma," *IEEE Transactions on Magnetics*, vol. 44, no. 6, pp. 978-981, 2008.
[21] J. Tang, G. Liu, and Q. Pan, "A Review on Representative Swarm Intelligence Algorithms for Solving Optimization Problems: Applications and Trends," *IEEE/CAA Journal of Automatica Sinica*, vol. 8, no. 10, pp. 1627-1643, 2021.
[22] A. Slowik, and H. Kwasnicka, "Nature Inspired Methods and Their Industry Applications—Swarm Intelligence Algorithms," *IEEE Transactions on Industrial Informatics*, vol. 14, no. 3, pp. 1004-1015, 2018.
[23] D. P. F. Cruz, R. D. Maia, and L. N. De Castro, "A critical discussion into the core of swarm intelligence algorithms," *Evolutionary Intelligence*, vol. 12, no. 2, pp. 189-200, 2019.

[24] M. M. Sabir, and T. Ali, "Optimal PID controller design through swarm intelligence algorithms for sun tracking system," *Applied Mathematics and Computation*, vol. 274, pp. 690-699, 2016.
[25] W.-T. Pan, "A new Fruit Fly Optimization Algorithm: Taking the financial distress model as an example," *Knowledge-Based Systems*, vol. 26, pp. 69-74, 2012.
[26] T. Bezdan, C. Stoean, A. A. Naamany, N. Bacanin, T. A. Rashid, M. Zivkovic, and K. Venkatachalam, "Hybrid Fruit-Fly Optimization Algorithm with K-Means for Text Document Clustering," *Mathematics*, vol. 9, no. 16, 1929, 2021.
[27] I. A. Ibrahim, M. J. Hossain, and B. C. Duck, "A hybrid wind driven-based fruit fly optimization algorithm for identifying the parameters of a double-diode photovoltaic cell model considering degradation effects," *Sustainable Energy Technologies and Assessments*, vol. 50, 101685, 2022.
[28] R. K. Poluru, and L. Kumar, "An Improved Fruit Fly Optimization (IFFOA) based Cluster Head Selection Algorithm for Internet of Things," *International Journal of Computers and Applications*, vol. 43, no. 7, pp. 623-631, 2019.
[29] H. Huang, X. A. Feng, S. Zhou, J. Jiang, H. Chen, Y. Li, and C. Li, "A new fruit fly optimization algorithm enhanced support vector machine for diagnosis of breast cancer based on high-level features," *BMC Bioinformatics*, vol. 20, no. 8, 1105, 2019.
[30] V. Solovyov, Z. Mendleson, and M. Takayasu, "Defect Tolerant High-Temperature Superconducting Cable for the Central Solenoid of Compact Fusion Reactor," *IEEE Transactions on Applied Superconductivity*, vol. 31, no. 5, pp. 1-5, 2021.
[31] T.-Y. Wu, A. Shao, and J.-S. Pan, "CTOA: Toward a Chaotic-Based Tumbleweed Optimization Algorithm," *Mathematics*, vol. 11, no. 10, 2339, 2023.
[32] T.-Y. Wu, H. Li, and S.-C. Chu, "CPPE: An Improved Phasmatodea Population Evolution Algorithm with Chaotic Maps," *Mathematics*, vol. 11, no. 9, 1977, 2023.
[33] L. Kang, R.-S. Chen, N. Xiong, Y.-C. Chen, Y.-X. Hu, and C.-M. Chen, "Selecting Hyper-Parameters of Gaussian Process Regression Based on Non-Inertial Particle Swarm Optimization in Internet of Things," *IEEE Access*, vol. 7, pp. 59504-59513, 2019.
[34] X. Yuan, X. Dai, J. Zhao, and Q. He, "On a novel multi-swarm fruit fly optimization algorithm and its application," *Applied Mathematics and Computation*, vol. 233, pp. 260-271, 2014.
[35] A. Darvish, and A. Ebrahimzadeh, "Improved Fruit-Fly Optimization Algorithm and Its Applications in Antenna Arrays Synthesis," *IEEE Transactions on Antennas and Propagation*, vol. 66, no. 4, pp. 1756-1766, 2018.
[36] L. Wang, Y. Shi, and S. Liu, "An improved fruit fly optimization algorithm and its application to joint replenishment problems," *Expert Systems with Applications*, vol. 42, no. 9, pp. 4310-4323, 2015.
[37] H. Iscan, and M. Gunduz, "Parameter Analysis on Fruit Fly Optimization Algorithm," *Journal of Computer and Communications*, vol. 02, no. 04, pp. 137-141, 2014.
[38] F. Marini, and B. Walczak, "Particle swarm optimization (PSO). A tutorial," *Chemometrics and Intelligent Laboratory Systems*, vol. 149, pp. 153-165, 2015.
[39] S. Das, S. S. Mullick, and P. N. Suganthan, "Recent advances in differential evolution – An updated survey," *Swarm and Evolutionary Computation*, vol. 27, pp. 1-30, 2016.